Actin polymerization driven by WASH causes V-ATPase retrieval and vesicle neutralization before exocytosis

Michael Carnell,[3] Tobias Zech,[3] Simon D. Calaminus,[3] Seiji Ura,[3] Monica Hagedorn,[1] Simon A. Johnston,[2] Robin C. May,[2] Thierry Soldati,[1] Laura M. Machesky,[3] and Robert H. Insall[3]

[1]Département de Biochimie, Faculté des Sciences II, Université de Genève, CH-1211 Genève 4, Switzerland
[2]School of Biosciences, University of Birmingham, Edgbaston, Birmingham B15 2TT, England, UK
[3]Cancer Research UK Beatson Institute for Cancer Research, Bearsden, Glasgow G61 1BD, Scotland, UK

WASP and SCAR homologue (WASH) is a recently identified and evolutionarily conserved regulator of actin polymerization. In this paper, we show that WASH coats mature *Dictyostelium discoideum* lysosomes and is essential for exocytosis of indigestible material. A related process, the expulsion of the lethal endosomal pathogen *Cryptococcus neoformans* from mammalian macrophages, also uses WASH-coated vesicles, and cells expressing dominant negative WASH mutants inefficiently expel *C. neoformans*. *D. discoideum* WASH causes filamentous actin (F-actin) patches to form on lysosomes, leading to the removal of vacuolar adenosine triphosphatase (V-ATPase) and the neutralization of lysosomes to form postlysosomes. Without WASH, no patches or coats are formed, neutral postlysosomes are not seen, and indigestible material such as dextran is not exocytosed. Similar results occur when actin polymerization is blocked with latrunculin. V-ATPases are known to bind avidly to F-actin. Our data imply a new mechanism, actin-mediated sorting, in which WASH and the Arp2/3 complex polymerize actin on vesicles to drive the separation and recycling of proteins such as the V-ATPase.

Introduction

Arp2/3 and nucleators

The Arp2/3 complex is normally inactive, but when it binds to nucleation-promoting factors (NPFs; Pollard, 2007), it becomes able to start new, growing actin filaments from the side of existing ones. Different NPFs initiate actin filaments in different locations. Most current research suggests that SCAR/WAVEs are principal drivers of lamellipodia and cell migration (Steffen et al., 2004), whereas WASPs usually regulate endocytosis and the formation of structures such as podosomes (Linder et al., 1999) and invadopodia (Yamaguchi et al., 2005). Recently, new families of NPFs have been discovered that generate actin at vesicular structures. WASP homologues associated with actin, membranes, and microtubules (Campellone et al., 2008) are important for Golgi function but are only found in vertebrates. The WASP and SCAR homologue (WASH), discovered as a gene in the subtelomeric region of human sex chromosomes, is essential for *Drosophila melanogaster* development through the larval stage (Linardopoulou et al., 2007).

WASH

WASH, like SCAR/WAVEs (Ibarra et al., 2005), is regulated as part of a protein complex (Gomez and Billadeau, 2009). As with SCAR/WAVE and its regulatory complex, there are few clues about its function from protein sequences; despite >200 kD of protein, there are no known domains outside the Arp2/3- and actin-binding WASH C terminus. The WASH complex is plainly important—all components are conserved, perhaps more widely than any other NPF (Veltman and Insall, 2010)—but surprisingly little is understood about its precise function. It has roles in at least two different retrograde vesicle traffic pathways in mammalian cells: fast recycling from early endosomes (Bear, 2009; Derivery et al., 2009; Duleh and Welch, 2010) and retromer-mediated transport from recycling endosomes (Gomez and Billadeau, 2009).

Correspondence to Robert H. Insall: R.Insall@beatson.gla.ac.uk

M. Hagedorn's present address is Bernhard Nocht Institute for Tropical Medicine, 20359 Hamburg, Germany.

Abbreviations used in this paper: NPF, nucleation-promoting factor; V-ATPase, vacuolar ATPase; WASH, WASP and SCAR homologue.

The Rockefeller University Press $30.00
J. Cell Biol. Vol. 193 No. 5 831–839
www.jcb.org/cgi/doi/10.1083/jcb.201009119

It binds directly to the retromer complex, associating it with retrograde flow from endosomes to the trans-Golgi network. RNAi of WASH in mammalian cells causes a hard to interpret phenotype involving the dispersal of endosomes containing the mannose 6–phosphate receptor and the tubulation of endosomal structures. The FAM21 complex subunit also associates with capping protein in mammals, suggesting a complex role in actin dynamics (Hernandez-Valladares et al., 2010).

Actin in *Dictyostelium discoideum* exocytosis

In this paper, we discuss the role of WASH in generating F-actin coats in *D. discoideum* lysosome maturation. *D. discoideum* growing in axenic medium have a well-defined endocytic cycle using most of the components seen in mammalian cells but with a far more rapid transit time. One difference is in lysosome maturation. Wild-type *D. discoideum* grows by phagocytosing bacteria; indigestible or inedible material is constitutively exocytosed between 90 and 120 min after endocytosis (Clarke et al., 2010). This process involves a small proportion of total vesicular traffic; most liquid is extracted from vesicles early in the cycle, and most membrane is recycled between the endosomal and lysosomal stages. Constitutive exocytosis is rarely seen in mammalian cells, presumably because of a combination of the lower rate of flux through the endolysosomal system and a greater range of retrograde pathways.

F-actin is polymerized on vesicles at two stages of the pathway. First, a fairly long-lived coat is seen between the lysosomal and postlysosomal stages (Drengk et al., 2003). A second phase of actin polymerization is seen immediately before neutralized vesicles are exocytosed (Clarke et al., 2010). By comparison, this is short lived, involving multiple dynamic flashes of F-actin, and only occurs in the 2–4 min before expulsion. This process is thought to position postlysosomes for exocytosis. In this manuscript, we show that WASH is essential for the first phase of actin polymerization during lysosome maturation and that this actin is essential for the neutralization and recycling of the vacuolar ATPase (V-ATPase).

Results and discussion

The *D. discoideum* WASH is well conserved, containing all the domains seen in human and *D. melanogaster* (Fig. 1 a), and, like WASP and SCAR, is encoded by a single gene. We generated several disruptants of the gene (*wshA*) in an AX2 background, giving identical phenotypes. *wshA*$^-$ mutants grew at near-normal rates in liquid medium, though we observed slower growth on bacteria (Fig. S1 a). They also showed no defects in cell migration, moving, if anything, faster than parental cells (Fig. S1 b). When *wshA*$^-$ cells were fixed and stained with phalloidin, there were also no visible changes in pseudopods or filopods at the leading edge. However, the large F-actin–coated intracellular vesicles seen in most normal cells were entirely absent from *wshA*$^-$ cells (Fig. 1 b). These do not colocalize with WASP or SCAR and are distinct from early endocytic actin structures such as phagosomes and macropinosomes, which are seen at normal levels. They have been previously observed using GFP fused to the actin-binding proteins ABP120 (Lee and Knecht, 2002) and coronin (Drengk et al., 2003) some time before indigestible material is exocytosed (Rauchenberger et al., 1997). These vesicles are present in >95% of normal cells but completely lost from *wshA*$^-$ cells (Fig. 1 c).

Expression of a GFP-WASH fusion in *wshA*$^-$ cells fully rescues the loss of these actin-coated vesicles (Fig. 1 d). The GFP-WASH and actin coats localize to the same vesicles (Fig. 1 d, green and red, respectively), suggesting that WASH directly induces the actin. We confirmed this using GFP-WASH in which the Arp2/3- and the actin-binding VCA domains have been deleted (Fig. 1 e, GFP-WASHΔVCA). This localizes normally to the large vesicles but does not rescue the actin coats, implying that the actin coats are directly generated by WASH acting as an NPF for the Arp2/3 complex.

Exocytosis is blocked in WASH mutants

We measured the rate of fluid phase uptake in *wshA*$^-$ cells using fluorescent dextran (Fig. 2 a). The initial rate of endocytosis was unaltered, although after incubations of >1 h, the *wshA*$^-$ cells accumulated significantly more dextran than the parent (Fig. 2 a, inset). Dextran is indigestible, and like the remains of food phagosomes (Clarke et al., 2002), it is normally exocytosed ∼1–2 h after passing through the endocytic and lysosomal pathways (Maniak, 2001; Neuhaus et al., 2002), leading to a plateau in accumulation. Therefore, this implies a defect in exocytosis rather than during earlier traffic. Thus, we measured the rate at which fluorescent dextran was expelled after loading. As shown in Fig. 2 b, whereas wild-type cells expelled nearly everything within 2 h, *wshA*$^-$ cells were completely unable to exocytose dextran (Fig. 2 b). Again, GFP-WASH rescued exocytosis near perfectly but had no effect when missing its VCA domain (Fig. 2 c). Thus, WASH-stimulated actin polymerization is essential for exocytosis. This has serious consequences to cells that encounter indigestible material (including, for example, bacterial cell walls; Clarke et al., 2002), presumably explaining the growth defect on bacteria. When cells were grown in 20% of 60-kD dextran, which barely affects normal cells, *wshA*$^-$ cells became extremely distended with large fluid-filled vesicles (Fig. 2 d) and divided far more slowly (Fig. 2 e).

We loaded cells with BSA 15-nm colloidal gold (Neuhaus et al., 2002), washed them for 2 h, and examined them by transmission EM (Fig. 2 f). Few wild-type cells contained BSA-containing vacuoles; those few were usually single, contained few gold particles, and were often empty or filled with low-density material (Fig. S1 c). However, 70% of the *wshA*$^-$ cells contained BSA-gold (Fig. 2 g), frequently at a high density and in densely stained vesicles. Single lysosomes often contained compacted deposits from several different endosomes, and fusion events were occasionally seen (Fig. 2 g), suggesting that the *wshA*$^-$ lysosomes are a dynamic "trash bin" containing the indigestible remains of multiple endosomes.

WASH in expulsion of *Cryptococcus neoformans* from macrophages

Constitutive exocytosis of endocytosed material is rare in mammals. To test the generality of this pathway, therefore,

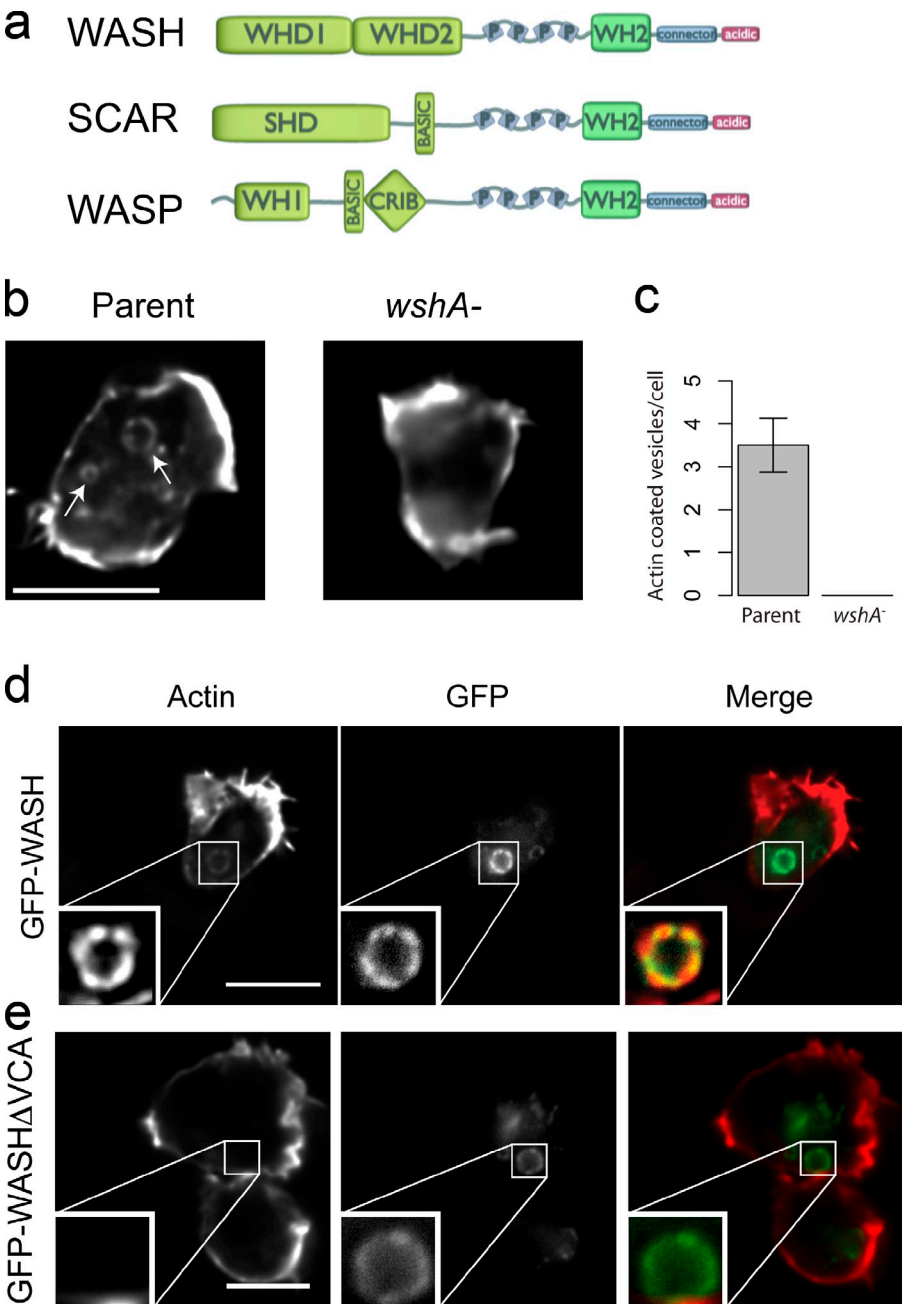

Figure 1. **WASH localizes to postlysosomes and is required for postlysosomal actin coats.** (a) Domain architecture of WASP subfamilies. (b) Deconvolved widefield images of parent (AX2) and WASH-null (*wshA*$^-$) cell lines fixed and stained with phalloidin. WASH-null cells lack large F-actin–coated vesicles (arrows in AX2). (c) Loss of actin-coated vesicles. Parental (n = 82) and *wshA*$^-$ (n = 79) cells were fixed and stained with phalloidin. Vesicles were counted in all planes of focus; macropinosomes were excluded. Error bars represent SEM. (d) Expression of GFP-WASH (middle panel and green) in fixed, phalloidin-stained (left panel and red) *wshA*$^-$ cells. (e) Expression of GFP-WASHΔVCA (green) in fixed, phalloidin-stained (left panel and red) *wshA*$^-$ cells. Bars, 10 µm.

we examined macrophages containing the pathogenic yeast *C. neoformans*, which is expelled from endosomes by a similar process (Alvarez and Casadevall, 2006; Ma et al., 2006) that is potentiated by chloroquine, implying a role for vesicle neutralization (Ma et al., 2006). Staining *C. neoformans*–laden J774 macrophages revealed a clear coat of WASH, similar to that seen in *D. discoideum* lysosomes, on the cytoplasmic face of the endosome, along with substantial accumulation of F-actin (Fig. 2 h). We did not obtain satisfactory RNAi in macrophages. However, we have found that expression of WASHΔVCA acts as a dominant negative in mammalian cells, for example by delaying recycling of transferrin (Fig. S2 a), but did not affect overall cell morphology or motility (not depicted). In macrophages, WASHΔVCA expression did not affect uptake of *C. neoformans* but caused a substantive block in expulsion (Fig. 2 i). Thus, WASH activity is important for *C. neoformans* expulsion in macrophages as well as *D. discoideum* postlysosomal exocytosis.

WASH- and actin-driven lysosome neutralization

When cells are loaded with a mixture of FITC- and TRITC-labeled dextran, neutral vesicles show yellow, but acidic vesicles are red because FITC loses fluorescence (Jenne et al., 1998). Most intracellular vesicles are acidic, but they neutralize as they mature to postlysosomes (Fig. 3 a, arrows). In *wshA*$^-$ cells, neutral postlysosomes were never seen. Again, this phenotype was fully rescued by GFP-WASH but not GFP-WASHΔVCA (Fig. 3 d). This suggests that *wshA*$^-$ cells cannot exocytose dextran because lysosomes are never able to neutralize and thus do not

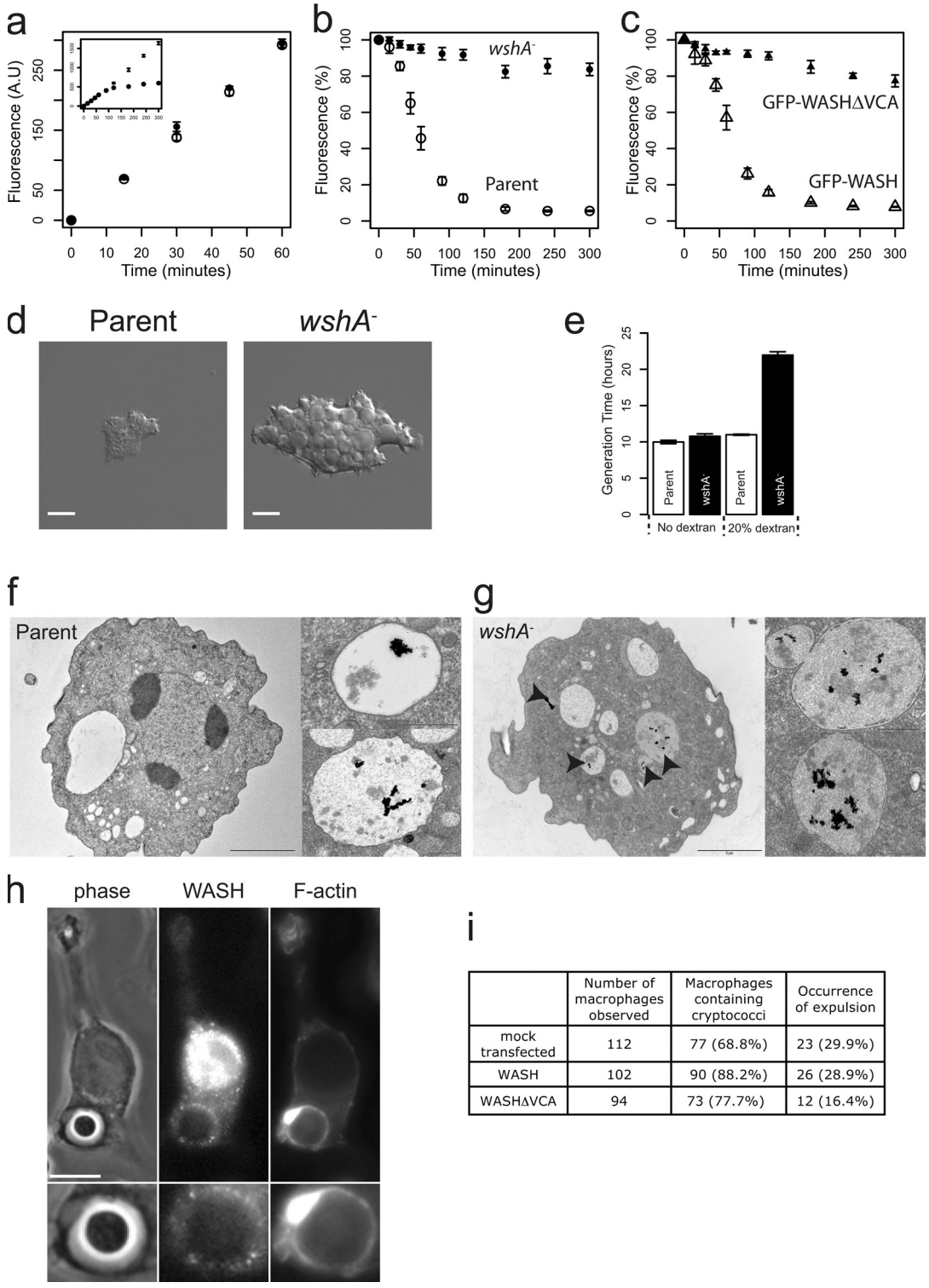

i

	Number of macrophages observed	Macrophages containing cryptococci	Occurrence of expulsion
mock transfected	112	77 (68.8%)	23 (29.9%)
WASH	102	90 (88.2%)	26 (28.9%)
WASHΔVCA	94	73 (77.7%)	12 (16.4%)

Figure 2. **WASH is required for exocytosis.** (a) Parental AX2 (○) and *wshA*⁻ (●) cells were incubated with FITC-dextran, and uptake was measured fluorimetrically. The inset shows a longer time course of the same data. (b and c) Parental AX2 (○), *wshA*⁻ cells (●), and *wshA*⁻ cells expressing GFP-WASH (△) and GFP-WASHΔVCA (▲) were loaded with FITC-dextran for 2 h and then washed. Expulsion of dextran was measured fluorimetrically. (d) Cells were grown for five generations in medium with 20% dextran. *wshA*⁻ cells, but not the parental strain, grew large and accumulated multiple dense vesicles. Bars, 5 µm. (e) Cells were grown for five generations in medium with and without 20% dextran. *wshA*⁻ growth is greatly slowed by the presence of indigestible dextran. (f and g) Transmission electron micrographs of parental AX2 (f) and *wshA*⁻ (g) cells incubated overnight with BSA–colloidal gold and chased for 2 h. Cells were examined as described in Hagedorn et al. (2009). Arrowheads in g indicate vesicular structures containing gold particles. Bars, 2 µm. (h) *C. neoformans*–containing vesicles in macrophages are also coated in WASH. Cultured J774 cells (left) were allowed to phagocytose *C. neoformans* and were then fixed with 4% formaldehyde and stained with anti-WASH (middle) and phalloidin (right). Bar, 10 µm. (i) Impairment of *C. neoformans* exocytosis caused by WASHΔVCA expression. Cells were transfected with full-length WASH or WASHΔVCA, incubated with *C. neoformans* for 2 h, and then observed for 24 h. The difference is significant to P = 0.05 (Fisher's exact test). Error bars in each case show the SD. *n* = 3 in each case in a–c and e.

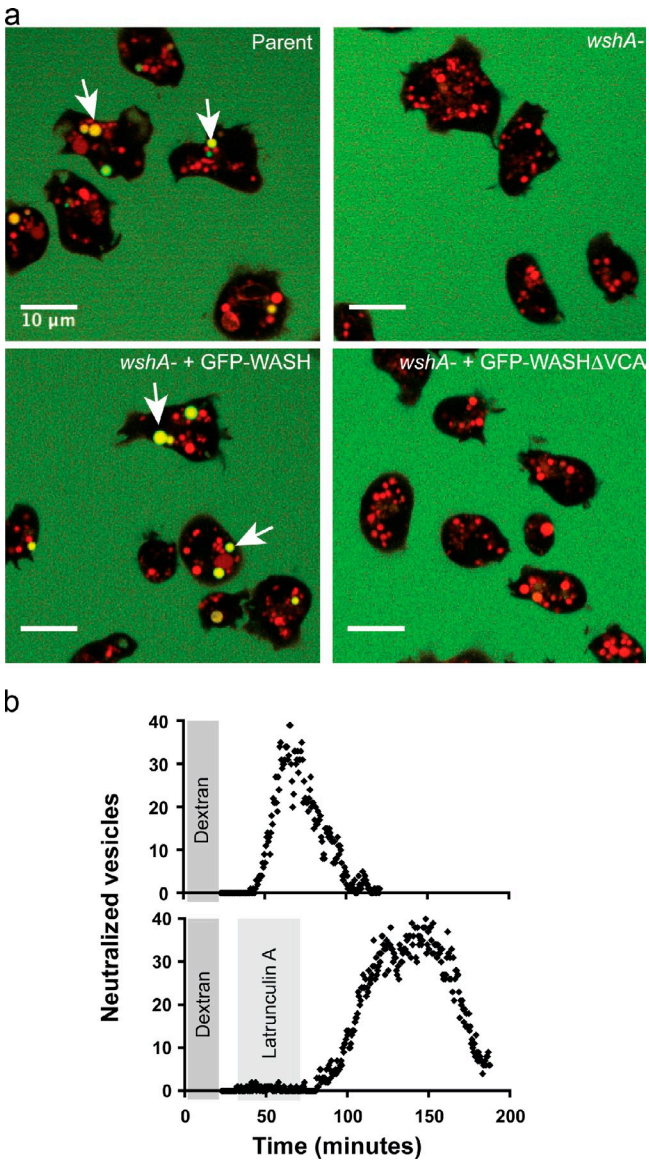

Figure 3. **WASH and actin polymerization are essential for vesicle neutralization.** (a) Vesicle neutralization assay. Cells were loaded with FITC- and TRITC-dextran to distinguish between acidic and neutral vesicles. Neutral postlysosomes (arrows) are absent from WASH-null cells and are rescued by expression of GFP-WASH but not GFP-WASHΔVCA (GFP is not seen under these conditions). (b) Latrunculin A completely but reversibly blocks the neutralization of vesicles. AX2 cells were loaded with a pulse of FITC-dextran, and the appearance of neutral vesicles was monitored in the presence or absence of 10 µg/ml latrunculin A. The figure shows measurements of Videos 1 and 2. The representative curves are from an experiment that was performed at least five times.

mature to postlysosomes. It also suggests that the role of WASH and the actin coat it generates is to mediate lysosome neutralization and maturation.

If this were true, lysosomal neutralization would be stopped by blocking actin polymerization. To test this hypothesis, we preloaded cells with FITC-dextran and counted the rate at which vesicles neutralized. As shown in Fig. 3 b and Video 1, vesicle neutralization started ~45 min after loading. We then used latrunculin A to block actin polymerization. To minimize secondary effects, latrunculin was only added from 40 min after loading, but this was still sufficient to block vesicle neutralization completely (Fig. 3 b and Video 2). The effect was rapidly reversible; washing away latrunculin allowed neutralization to restart within a few minutes. Thus, actin polymerization is essential for vesicle neutralization.

WASH and V-ATPase recycling

The V-ATPase, which consists of a membrane channel (V_0) and a cytoplasmic ATP-hydrolyzing proton pump (V_1; Jefferies et al., 2008), mediates vesicle acidification. When it is removed, vesicles neutralize through proton leaks. It has been known for several years that subunits of V_1 have a surprisingly high affinity for actin. Each V_1 contains three B subunits, which have a submicromolar affinity for F-actin (Holliday et al., 2000), and the single C subunit also binds actin (Vitavska et al., 2003). Together, these imply an extremely high avidity for F-actin. We hypothesized that the WASH-derived F-actin coat on lysosomes was neutralizing them by binding and removing the V-ATPase. This was supported by coimmunoprecipitation from detergent lysates (Fig. S3). VatM and VatB subunits (from V_0 and V_1, respectively) were identified with 100% confidence from GFP-WASH pull-downs but not from GFP alone (Fig. S3). Thus, WASH can physically associate with V-ATPase either directly or as part of a larger protein assembly. However, our data suggest that this interaction results in V-ATPase recycling and is thus short lived. We simultaneously imaged VatB-RFP and GFP-WASH in cells that had been fed ~2-µm indigestible agarose beads, which made lysosomes large enough that they could be imaged continuously. As seen in Fig. 4 a and Video 3, the V_1 subunit began disappearing from the lysosome as soon as puncta of GFP-WASH appeared. Quantitation shows V-ATPase levels start to drop within 1 or 2 min of the arrival of WASH (Fig. 4 b). Unexpectedly, however, WASH was only present in puncta, whereas the V-ATPase was removed; all detectable V-ATPase had gone well before formation of the contiguous coat of WASH seen on postlysosomes.

In yeast, V-ATPase is inactivated by dissociation of V_1 from the V_0 subunit (Parra and Kane, 1998), though it is unclear how universal this mechanism is for metazoans. Therefore, we examined GFP-tagged VatM, a V_0 subunit (Fig. 4 c), but both halves are recycled at a similar stage. The neutralization mediated by WASH, therefore, is not caused by a yeast-like mechanism in which V_1 is removed and V_0 is left on the vesicle. The implication is that the *D. discoideum* V-ATPase is recycled as an intact complex, but we have been unable to test this directly, as GFP-V_1 and RFP-V_0 appear to be impossible to coexpress. GFP-coronin, a marker for actin and the presence of the dynamic Arp2/3 complex (Humphries et al., 2002), was recruited around the same time as WASH. GFP fused to vacuolin A, the *D. discoideum* flotillin homologue (Wienke et al., 2006), accumulated earlier than WASH (Fig. 4 b). This was surprising, as recruitment of vacuolin was thought to occur at the stage when lysosomes mature to postlysosomes (Rauchenberger et al., 1997; Jenne et al., 1998). Our data suggest that vacuolin is recruited more gradually, before the formation of postlysosmes, and that WASH and WASH-induced actin are in fact the best available markers for the transition between

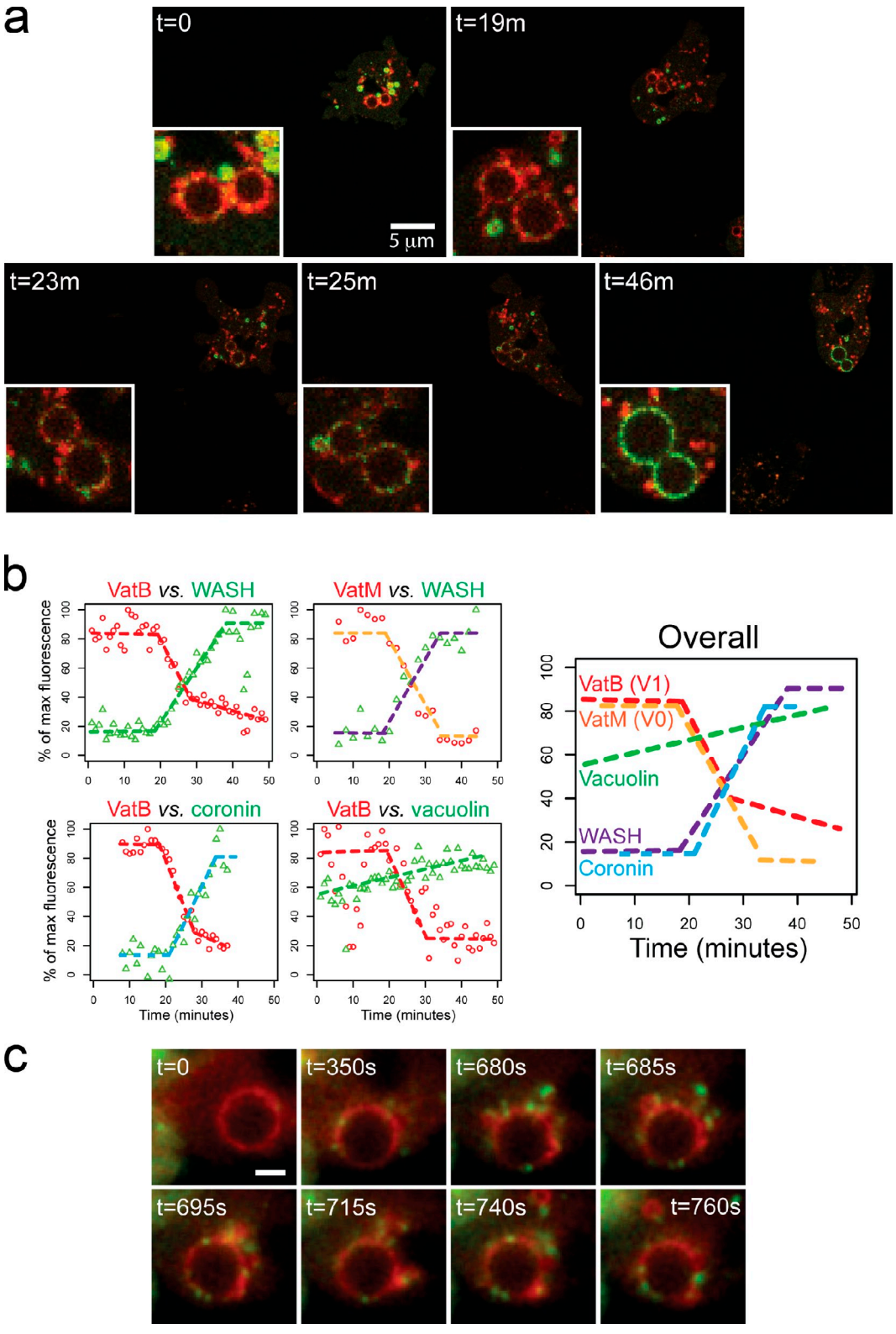

Figure 4. **WASH causes recycling of the V-ATPase.** (a) Confocal imaging of *wshA*$^{-}$ cells expressing GFP-WASH and VatB-mRFP after endocytosis of 0.5-µm agarose beads. Frames are taken from Video 3. Insets show a magnified view of the vesicle on which WASH is acting. (b) Quantification of various vesicular proteins during postlysosome formation. Graphs show that the loss of V-ATPase immediately follows the arrival of WASH and coronin, whereas the previously described (Maniak, 2001) postlysosome marker vacuolin is present much earlier than neutralization and rises steadily. The representative curves are from an experiment that was performed at least five times. (c) Rapid widefield oblique illumination imaging of small vesicles containing both GFP-WASH and VatB-mRFP budding a single lysosome. Frames are taken from Video 4. Bar, 1 µm.

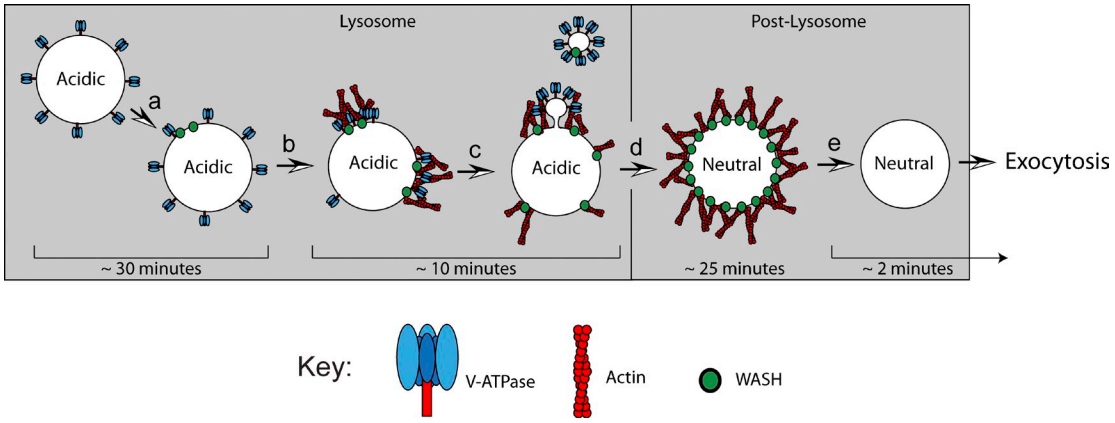

Figure 5. **The role of WASH and actin in lysosome neutralization.** A schematic diagram of the model proposed in this paper: (a) WASH recruited to acidic lysosomes; (b) WASH puncta cause local actin polymerization, and F-actin binds to V-ATPase; (c) small recycling vesicles bud off, and V-ATPase is recruited by WASH/F-actin; (d) loss of V-ATPase causes the vesicle to neutralize and mature to postlysosome; (e) WASH is removed some time after neutralization.

acidic lysosomes and neutral postlysosomes. To confirm this, we stained *wshA*$^-$ cells with antivacuolin; the acidic lysosomes of the *wshA*$^-$ cells accumulated normal levels (Fig. S1 f), confirming that WASH is not involved in vacuolin recruitment.

We imaged the beads at the highest possible spatial and temporal resolution (Fig. 4 c and Video 4). Lysosomes were relatively quiescent before the appearance of WASH. Soon after puncta of GFP-WASH were first visible, corrugations appeared on the edge of the lysosomes, and small vesicles containing puncta of both GFP-WASH and VatB-mRFP budded off. These vesicles are apparently the V-ATPase recycling vesicles predicted by previous work (Clarke et al., 2002) and were recently directly observed (Clarke et al., 2010). Our results show that these vesicles require WASH to function.

Altogether, our data show that the role of WASH in *D. discoideum* is to cause new actin polymerization on mature lysosomes, and the role of this F-actin is to bind to the V-ATPase and sort it to recycling vesicles (Fig. 5). This allows the lysosome to neutralize before being exocytosed. In the absence of WASH, the V-ATPase remains on the lysosome, which therefore remains acidic, immature, and unable to exocytose.

The importance of actin to vesicle traffic is becoming increasingly clear (Qualmann and Kessels, 2002). Our work suggests that WASH, by sequestering vesicular proteins and connecting them to recycling vesicles, is a principal contributor. Our work raises several questions, in particular how the cells survive an apparently total block in their exocytic pathways.

The block in exocytosis in *wshA*$^-$ mutants is near total, but only a very small proportion of either fluid or membrane is normally exocytosed. Most fluid is removed along with nutrients early in the endocytic pathway. Nearly all of the membrane is also recovered (Gotthardt et al., 2002), as shown in Fig. 4. The accumulated lysosomes represent a very small fraction of the total throughput of the membrane. In cells not grown in indigestible material, the fraction is presumably even smaller. Thus, loss of WASH causes a relatively slight growth defect for cells grown in axenic medium. Indigestible material (from bacteria or dextran in the medium) ties up more of both and thus causes a serious growth defect.

The vesicle traffic and recycling pathways of metazoa are more complex than those of *D. discoideum*. However, it seems likely that the underlying physiological role is consistent. The functions of other NPFs are conserved across species. RNAi of WASH from mammalian cells causes a much less emphatic phenotype involving two or more recycling pathways at different stages of endocytic transport (Derivery et al., 2009; Gomez and Billadeau, 2009), but each step involves retrograde pathways, thus requiring neutralization. Although constitutive exocytosis of the *D. discoideum* kind is unusual in mammals, the example we have tested, the expulsion of *C. neoformans*, requires WASH, and expression of WASH-ΔVCA also altered the pattern of V-ATPase recruitment and recycling in *C. neoformans*–fed macrophages (Fig. S2 b), again implying that these pathways are conserved.

Actin-mediated sorting

Overall, our data imply that the role of WASH and the Arp2/3 complex is to perform actin-mediated sorting, generating F-actin to sequester and remove specific proteins from vesicles. The V-ATPase has a particularly strong avidity for F-actin, but many other recycled proteins—in particular, growth factor receptors—have unexplained actin-binding activities that may in fact be tags for actin-mediated sorting. Furthermore, the unusually clear, experimentally tractable phenotype we see in *D. discoideum* will enable genetic dissection of WASH function that would be impossible given the subtle phenotypes seen in mammalian cells.

Materials and methods

Cell culture and growth assessment

D. discoideum cells were grown at RT in HL5 medium plus glucose (Formedium) either in Petri dishes or shaken in flasks. All subsequent experiments and imaging were also performed at RT. Measurement of generation time was performed in shaken culture with and without 20% dextran (wt/vol, molecular mass = 60–90 kD), with samples taken periodically and analyzed for population density and cell size distribution using a cell counter (CASY; Roche). Cultures exceeding 2 × 10^6 cells/ml were diluted to 10^5 cells/ml. After 4 d of growth, differential interference contrast images of those cells that adhered to glass-bottomed dishes were taken using a microscope (TE2000-E; Nikon) with a 60× 1.4 NA objective fitted with a

camera (Retiga EXi; QImaging) and captured using µManager 1.3 software (Micro-Manager).

Gene disruption

D. discoideum WASH-null cell lines were generated by targeted gene disruption using homologous recombination. A plasmid was constructed containing a floxed Blasticidin resistance cassette flanked with regions homologous to genes upstream (dictyBase database accession no. DDB_G0292876) and downstream (dictyBase database accession no. DDB_G0292972) of WASH (dictyBase database accession no. DDB_G0292878). This construct was linearized and electroporated into AX2 cells. Blasticidin-resistant cells were screened by Western blotting using a peptide anti-WASH antibody (BioGenes GmbH) for loss of WASH.

Fluorescent fusion proteins

Exogenously expressed proteins were cloned from cDNA by PCR. WASH and related genes were cloned into the extrachromosomal GFP fusion expression plasmid pDM351 (Veltman et al., 2009). vatM and vatB (without a stop codon) were cloned into mRFPmars shuttle vectors pDM411 and pDM413, respectively (Veltman et al., 2009). These were then excised and inserted into a GFP-WASH extrachromosomal vector to create dual expression constructs.

Cell fixation

Cells were seeded onto coverslips and allowed to adhere for 30 min. They were then fixed with 2% (wt/vol) formaldehyde, 15% (vol/vol) saturated picric acid, and 10 mM Pipes, pH 6.5, for 15 min (Hagedorn et al., 2009). Coverslips were washed in PBS before postfixation for 2 min with 70% ethanol followed by sequential washes in PBS glycine. Cells were incubated with 33 nm Texas red phalloidin (Invitrogen) in PBS for 1 h. Coverslips were washed in PBS and mounted on glass slides using antifade reagent (Prolong Gold; Invitrogen). Cells were imaged using an inverted widefield microscope (IX81; Olympus) moved by a piezoelectric stage using a 100× 1.4 NA objective. Images were captured with a camera (CoolSnap HQ2; Photometrics) using Volocity software (PerkinElmer). Iterative deconvolution was performed with a calculated point spread function using Volocity 3D image restoration software. Image contrast was adjusted using ImageJ software (National Institutes of Health).

Endocytosis/exocytosis assays

Rates of endocytosis and exocytosis were assessed by measuring the intracellular level of FITC-dextran after its addition or removal from HL5 growth medium, respectively. For measuring rates of endocytosis, cells were suspended in 10 ml HL5 medium at 10^6 cells/ml and shaken at 120 rpm. Samples were taken to measure protein content before the start of the experiment to normalize results between replicas. 20 mg FITC-dextran was added to flasks, and 500-µl samples were taken at 0-, 15-, 30-, 45-, 60-, 90-, 120-, 180-, 240-, and 300-min time points. To measure exocytosis, 10-ml cultures at 5×10^6 cells/ml were incubated overnight with 20 mg FITC-dextran. Cells were pelleted and suspended in fresh HL5 medium, and samples were taken at the aforementioned time points. Samples were washed in ice-cold KK2 buffer and pelleted. Pellets were lysed in 50 mM Na_2HPO_4, pH 9.3, and 0.2% Triton X-100 and measured on a fluorimeter (470-nm excitation and 515-nm emission; Photon Technology International).

Postlysosome visualization

Visualization of *D. discoideum* postlysosomes was performed using FITC- and TRITC-conjugated dextran as previously described by Rivero and Maniak (2006) and Jenne et al. (1998). Cells were seeded onto glass-bottomed dishes and incubated in LoFlo medium (Formedium) containing 4 mg/ml FITC-dextran and 40 mg/ml TRITC-dextran. After 1 h, dishes were imaged on a Nikon A1 confocal microscope (FITC, 488-nm excitation and 500–550-nm emission; TRITC, 561.4-nm excitation and 570–620-nm emission) with a 60× 1.4 NA objective. Laser power and photomultiplier tube voltage were adjusted based on wild-type AX2 cells so that acidic lysosomes and neutral postlysosomes could be visually distinguished. These settings were not changed between subsequent cell types or dishes. Images were acquired using NIS-Elements AR3.1 software (Nikon).

FITC-dextran pulse chase

Wild-type AX2 cells were briefly incubated in LoFlo medium containing 4 mg/ml FITC for 20 min, after which the dish was rinsed twice with fresh LoFlo medium. After the pulse period, the dish was imaged by time-lapse microscopy on a widefield fluorescence microscope (Olympus) at low magnification (40× 0.75 NA objective) using a camera (QuantEM; Photometrics). Latrunculin A (EMD) was added to the dish at a final concentration of 2 µM at various times during imaging. For washout experiments, the dish was removed from the microscope, rinsed twice with fresh LoFlo medium, and immediately returned to the microscope. Images were acquired using Volocity software, and postlysosomes were quantified with ImageJ using its built-in Analyze Particles routine.

Live cell imaging

For imaging of cells expressing fluorescent fusion proteins, cells were placed in LoFlo medium at least 2 h before imaging. Cells were incubated for 20 min with agarose beads and then compressed under a layer of 1% (wt/vol) agarose made using LoFlo medium. For quantitative microscopy, cells were imaged on an A1 confocal microscope (GFP, 488-nm excitation and 500–550-nm emission; mRFP, 561.4-nm excitation and 570–620-nm emission) with a 60× 1.4 NA objective. For qualitative high speed acquisition, cells were imaged on a TE2000-U widefield microscope with a 100× 1.49 NA objective, with illumination provided by 473- and 561-nm solid-state lasers (Deepstar; Omicron Laserage Laserprodukte GmbH). Images were captured with a camera (Cascade II; Photometrics) using Metamorph version 7 software (Universal Imaging). ImageJ was used for the quantification of fluorescence around phagocytosed particles using a doughnut-shaped region of interest to obtain mean intensity.

C. neoformans expulsion

RAW macrophages transiently expressing WASH or WASHΔVCA were incubated with opsonised (1.98 µg/10^6 cells/100 µl, 1 h rotating at RT) *C. neoformans* strain H99-GFP (Voelz et al., 2010) for 2 h. After phagocytosis of *Cryptococci*, J774 macrophage cells were washed three times in DME without phenol red. Cells were imaged on a microscope (TE2000) enclosed in a temperature-controlled and humidified environmental chamber (okolab) with 5% CO_2 at 37°C. Time-lapse images were captured with a camera (Digital Sight DS-Qi1MC; Nikon) with a 20× objective (Ph1 PLAN APO 0.45 NA) using NIS-Elements AR software. Fluorescence and phase-contrast images were captured every 2 min for 24 h. The occurrence of expulsion was analyzed as described previously (Ma et al., 2006).

WASH and V-ATPase localization on *C. neoformans*–containing phagosomes

J774 macrophages were fixed with formaldehyde 3 h after phagocytosis of *C. neoformans* and incubation at 5% CO_2 and 37°C. After fixation, cells were labeled with anti-WASH antibody and TRITC phalloidin. RAW macrophages transiently expressing WASH or WASHΔVCA were fixed with formaldehyde at the time points indicated after phagocytosis of *C. neoformans* and were labeled with anti-ATP6V1B2. Images were captured using a Digital Sight DS-Qi1MC camera with a 60× objective (PLAN APO 1.4 NA) using NIS-Elements AR software. The A1R confocal used in this research was obtained through Birmingham Science City Translational Medicine Clinical Research and Infrastructure Trials Platform with support from Advantage West Midlands.

Online supplemental material

Fig. S1 shows bacterial growth, migration, and EM of *D. discoideum*. Fig. S2 shows V-ATPase localization in *C. neoformans*–infected macrophages, and Fig. S3 shows the identification of proteins associated with GFP-WASH. Videos 1 and 2 show the neutralization of vesicles in untreated cells and after latrunculin, respectively. Video 3 shows WASH association and V-ATPase removal from vesicles, and Video 4 shows the detail of a single lysosome during neutralization. Online supplemental material is available at http://www.jcb.org/cgi/content/full/jcb.201009119/DC1.

We are grateful to Margaret Clarke, Nia Bryant, Douwe Veltman, Jason King, and Laura Park for discussions, to Margaret O'Prey for assistance with imaging, and to Willy Bienvenut, David Sumpton, and Sergio Lilla for mass spectrometry.

This work was supported by core Cancer Research UK grants to R.H. Insall and L.M. Machesky, by the Deutsche Forschungsgemeinschaft and the Swiss National Science Foundation, by the Wellcome Trust (088148MF), and by a Lister Research Prize Fellowship to R.C. May.

Submitted: 24 September 2010
Accepted: 25 April 2011

References

Alvarez, M., and A. Casadevall. 2006. Phagosome extrusion and host-cell survival after *Cryptococcus neoformans* phagocytosis by macrophages. *Curr. Biol.* 16:2161–2165. doi:10.1016/j.cub.2006.09.061

Bear, J.E. 2009. Sorting out endosomes in the WASH. *Dev. Cell*. 17:583–584. doi:10.1016/j.devcel.2009.10.019

Campellone, K.G., N.J. Webb, E.A. Znameroski, and M.D. Welch. 2008. WHAMM is an Arp2/3 complex activator that binds microtubules and functions in ER to Golgi transport. *Cell*. 134:148–161. doi:10.1016/j.cell.2008.05.032

Clarke, M., J. Köhler, Q. Arana, T. Liu, J. Heuser, and G. Gerisch. 2002. Dynamics of the vacuolar H(+)-ATPase in the contractile vacuole complex and the endosomal pathway of *Dictyostelium* cells. *J. Cell Sci.* 115:2893–2905.

Clarke, M., L. Maddera, U. Engel, and G. Gerisch. 2010. Retrieval of the vacuolar H-ATPase from phagosomes revealed by live cell imaging. *PLoS ONE*. 5:e8585. doi:10.1371/journal.pone.0008585

Derivery, E., C. Sousa, J.J. Gautier, B. Lombard, D. Loew, and A. Gautreau. 2009. The Arp2/3 activator WASH controls the fission of endosomes through a large multiprotein complex. *Dev. Cell*. 17:712–723. doi:10.1016/j.devcel.2009.09.010

Drengk, A., J. Fritsch, C. Schmauch, H. Rühling, and M. Maniak. 2003. A coat of filamentous actin prevents clustering of late-endosomal vacuoles in vivo. *Curr. Biol.* 13:1814–1819. doi:10.1016/j.cub.2003.09.037

Duleh, S.N., and M.D. Welch. 2010. WASH and the Arp2/3 complex regulate endosome shape and trafficking. *Cytoskeleton (Hoboken)*. 67:193–206.

Gomez, T.S., and D.D. Billadeau. 2009. A FAM21-containing WASH complex regulates retromer-dependent sorting. *Dev. Cell*. 17:699–711. doi:10.1016/j.devcel.2009.09.009

Gotthardt, D., H.J. Warnatz, O. Henschel, F. Brückert, M. Schleicher, and T. Soldati. 2002. High-resolution dissection of phagosome maturation reveals distinct membrane trafficking phases. *Mol. Biol. Cell*. 13:3508–3520. doi:10.1091/mbc.E02-04-0206

Hagedorn, M., K.H. Rohde, D.G. Russell, and T. Soldati. 2009. Infection by tubercular mycobacteria is spread by nonlytic ejection from their amoeba hosts. *Science*. 323:1729–1733. doi:10.1126/science.1169381

Hernandez-Valladares, M., T. Kim, B. Kannan, A. Tung, A.H. Aguda, M. Larsson, J.A. Cooper, and R.C. Robinson. 2010. Structural characterization of a capping protein interaction motif defines a family of actin filament regulators. *Nat. Struct. Mol. Biol.* 17:497–503. doi:10.1038/nsmb.1792

Holliday, L.S., M. Lu, B.S. Lee, R.D. Nelson, S. Solivan, L. Zhang, and S.L. Gluck. 2000. The amino-terminal domain of the B subunit of vacuolar H+-ATPase contains a filamentous actin binding site. *J. Biol. Chem.* 275:32331–32337. doi:10.1074/jbc.M004795200

Humphries, C.L., H.I. Balcer, J.L. D'Agostino, B. Winsor, D.G. Drubin, G. Barnes, B.J. Andrews, and B.L. Goode. 2002. Direct regulation of Arp2/3 complex activity and function by the actin binding protein coronin. *J. Cell Biol.* 159:993–1004. doi:10.1083/jcb.200206113

Ibarra, N., A. Pollitt, and R.H. Insall. 2005. Regulation of actin assembly by SCAR/WAVE proteins. *Biochem. Soc. Trans.* 33:1243–1246. doi:10.1042/BST20051243

Jefferies, K.C., D.J. Cipriano, and M. Forgac. 2008. Function, structure and regulation of the vacuolar (H+)-ATPases. *Arch. Biochem. Biophys.* 476:33–42. doi:10.1016/j.abb.2008.03.025

Jenne, N., R. Rauchenberger, U. Hacker, T. Kast, and M. Maniak. 1998. Targeted gene disruption reveals a role for vacuolin B in the late endocytic pathway and exocytosis. *J. Cell Sci.* 111:61–70.

Lee, E., and D.A. Knecht. 2002. Visualization of actin dynamics during macropinocytosis and exocytosis. *Traffic*. 3:186–192. doi:10.1034/j.1600-0854.2002.030304.x

Linardopoulou, E.V., S.S. Parghi, C. Friedman, G.E. Osborn, S.M. Parkhurst, and B.J. Trask. 2007. Human subtelomeric WASH genes encode a new subclass of the WASP family. *PLoS Genet.* 3:e237. doi:10.1371/journal.pgen.0030237

Linder, S., D. Nelson, M. Weiss, and M. Aepfelbacher. 1999. Wiskott-Aldrich syndrome protein regulates podosomes in primary human macrophages. *Proc. Natl. Acad. Sci. USA*. 96:9648–9653. doi:10.1073/pnas.96.17.9648

Ma, H., J.E. Croudace, D.A. Lammas, and R.C. May. 2006. Expulsion of live pathogenic yeast by macrophages. *Curr. Biol.* 16:2156–2160. doi:10.1016/j.cub.2006.09.032

Maniak, M. 2001. Fluid-phase uptake and transit in axenic *Dictyostelium* cells. *Biochim. Biophys. Acta*. 1525:197–204.

Neuhaus, E.M., W. Almers, and T. Soldati. 2002. Morphology and dynamics of the endocytic pathway in *Dictyostelium discoideum*. *Mol. Biol. Cell*. 13:1390–1407. doi:10.1091/mbc.01-08-0392

Parra, K.J., and P.M. Kane. 1998. Reversible association between the V1 and V0 domains of yeast vacuolar H+-ATPase is an unconventional glucose-induced effect. *Mol. Cell. Biol.* 18:7064–7074.

Pollard, T.D. 2007. Regulation of actin filament assembly by Arp2/3 complex and formins. *Annu. Rev. Biophys. Biomol. Struct.* 36:451–477. doi:10.1146/annurev.biophys.35.040405.101936

Qualmann, B., and M.M. Kessels. 2002. Endocytosis and the cytoskeleton. *Int. Rev. Cytol.* 220:93–144. doi:10.1016/S0074-7696(02)20004-2

Rauchenberger, R., U. Hacker, J. Murphy, J. Niewöhner, and M. Maniak. 1997. Coronin and vacuolin identify consecutive stages of a late, actin-coated endocytic compartment in *Dictyostelium*. *Curr. Biol.* 7:215–218. doi:10.1016/S0960-9822(97)70093-9

Rivero, F., and M. Maniak. 2006. Quantitative and microscopic methods for studying the endocytic pathway. *Methods Mol. Biol.* 346:423–438.

Steffen, A., K. Rottner, J. Ehinger, M. Innocenti, G. Scita, J. Wehland, and T.E. Stradal. 2004. Sra-1 and Nap1 link Rac to actin assembly driving lamellipodia formation. *EMBO J.* 23:749–759. doi:10.1038/sj.emboj.7600084

Veltman, D.M., and R.H. Insall. 2010. WASP family proteins: their evolution and its physiological implications. *Mol. Biol. Cell*. 21:2880–2893. doi:10.1091/mbc.E10-04-0372

Veltman, D.M., G. Akar, L. Bosgraaf, and P.J. Van Haastert. 2009. A new set of small, extrachromosomal expression vectors for *Dictyostelium discoideum*. *Plasmid*. 61:110–118. doi:10.1016/j.plasmid.2008.11.003

Vitavska, O., H. Wieczorek, and H. Merzendorfer. 2003. A novel role for subunit C in mediating binding of the H+-V-ATPase to the actin cytoskeleton. *J. Biol. Chem.* 278:18499–18505. doi:10.1074/jbc.M212844200

Voelz, K., S.A. Johnston, J.C. Rutherford, and R.C. May. 2010. Automated analysis of *cryptococcal* macrophage parasitism using GFP-tagged *cryptococci*. *PLoS ONE*. 5:e15968. doi:10.1371/journal.pone.0015968

Wienke, D., A. Drengk, C. Schmauch, N. Jenne, and M. Maniak. 2006. Vacuolin, a flotillin/reggie-related protein from *Dictyostelium* oligomerizes for endosome association. *Eur. J. Cell Biol.* 85:991–1000. doi:10.1016/j.ejcb.2006.04.010

Yamaguchi, H., M. Lorenz, S. Kempiak, C. Sarmiento, S. Coniglio, M. Symons, J. Segall, R. Eddy, H. Miki, T. Takenawa, and J. Condeelis. 2005. Molecular mechanisms of invadopodium formation: the role of the N-WASP-Arp2/3 complex pathway and cofilin. *J. Cell Biol.* 168:441–452. doi:10.1083/jcb.200407076